Chinese Chemical Letters 33 (2022) 979–982

Contents lists available at ScienceDirect

Chinese Chemical Letters

journal homepage: www.elsevier.com/locate/cclet

Construction of high stability indium gallium zinc oxide transistor biosensors for reliable detection of bladder cancer-associated microRNA

Jing Guo[a], Ruichen Shen[c], Xuejie Shen[c], Bo Zeng[a], Nianjun Yang[d], Huageng Liang[b,*], Yanbing Yang[a,*], Quan Yuan[a,c,*]

[a] Key Laboratory of Biomedical Polymers of Ministry of Education, College of Chemistry and Molecular Sciences, School of Microelectronics, Wuhan University, Wuhan 430072, China
[b] Department of Urology, Union Hospital, Tongji Medical College, Huazhong University of Science and Technology, Wuhan 430022, China
[c] Institute of Chemical Biology and Nanomedicine, State Key Laboratory of Chemo/Biosensing and Chemometrics, College of Chemistry and Chemical Engineering, Hunan University, Changsha 410082, China
[d] Institute of Materials Engineering, University of Siegen, Siegen 57076, Germany

ARTICLE INFO

Article history:
Received 29 April 2021
Revised 6 July 2021
Accepted 19 July 2021
Available online 26 July 2021

Keywords:
Bladder cancer
Field-effect transistors
IGZO
miRNA
Urine

ABSTRACT

Bladder cancer is the most common malignant tumours with high morbidity, mortality and recurrence. However, currently developed detection methods for bladder cancer-associated urine biomarkers are hindered by their extremely low abundance. Hence, the exploration of a highly sensitive and selective approach for the detection of trace bladder cancer-associated biomarkers in human urine is of vital importance for the diagnosis of bladder cancer. Herein, we developed a highly reliable indium gallium zinc oxide field effect transistor (IGZO FET) biosensor for the detection of bladder cancer-related biomarker microRNA. The single-stranded DNA-functionalized IGZO FET biosensors exhibit high sensing reproducibility and stability with an ultralow detection limit of 19.8 amol/L. The device could also be used for quantitative detection of trace microRNA in human urine samples and can effectively distinguish bladder cancer patients from healthy donors. The development of high performance IGZO FET biosensors presents new opportunities for the achievement of early-stage diagnosis of bladder cancer.

Bladder cancer is one of the most common malignant tumours in the urinary system with a high and rising trend of mortality [1–3]. Timely diagnosis of early-stage bladder cancer remains the contributing bottleneck due to its complex pathological types and nonspecific symptoms [4,5]. Urine, as the metabolic microenvironment of bladder tumour cells, contains abundant bladder cancer biomarkers, providing an alternative strategy for non-invasive diagnosis of bladder cancer [6,7]. Currently, researchers have identified numerous types of bladder cancer biomarkers in urine including DNA [8], RNA [9], proteins [10,11], tumour cells [12] and metabolites [13]. Particularly, microRNA (miRNA) plays a crucial role in cell metastasis, development, proliferation, apoptosis and carcinogenesis, and it was immediately excreted into urine *via* the metabolism of bladder tumour cells in case of bladder carcinogenesis [14–16]. Therefore, the quantitative detection of bladder cancer-associated miRNA in human urine is an effective strategy to achieve non-invasive diagnosis of early-stage bladder cancer. However, currently developed bladder cancer urine biomarkers diagnosis methods are hindered by low detection reliability due to extremely low abundance of bladder cancer-related miRNA in complex urine environments [17,18]. Consequently, the exploration of a highly reliable approach for the detection of trace miRNA in human urine is of vital importance for the diagnosis and postoperative of bladder cancer.

Nano-biosensors constructed by nanomaterials have been comprehensively employed for the detection of disease-relevant biomarkers [19–21]. As a type of nano-biosensors, field effect transistors (FETs) exhibit prominent electrical performance, ease to be miniaturized and integrated [22,23]. Owing to its intrinsic amplification feature, FET biosensors could generate a significant electrical signal response under a tiny local microenvironment change, therefore demonstrating tremendous potential in highly sensitive detection of disease-relevant biomarkers. In the FET biosensors, semiconductor channel nanomaterials play a central role in the

* Corresponding authors.
E-mail addresses: leonard19800318@hust.edu.cn (H. Liang), yangyanbing@whu.edu.cn (Y. Yang), yuanquan@whu.edu.cn (Q. Yuan).

https://doi.org/10.1016/j.cclet.2021.07.048
1001-8417/

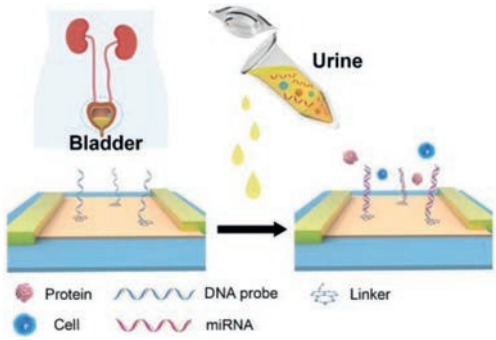

Scheme 1. Schematic illustration of ssDNA-IGZO biosensors for miRNA detection.

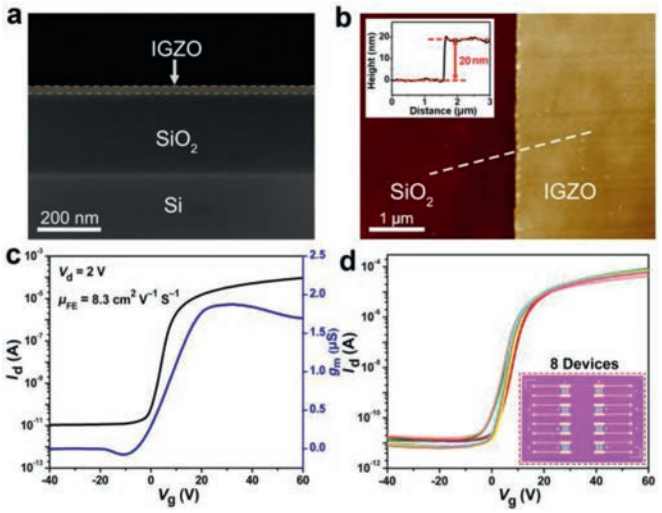

Fig. 1. (a) Cross-section SEM image and (b) AFM image of IGZO channel. Inset of (b), Corresponding quantitative height profile of IGZO channel. (c) Transfer characteristics and transconductance of IGZO FET at V_d = 2 V. (d) Performance stability of eight IGZO FETs at V_d = 2 V. Inset: Photograph of a IGZO FET.

determination of device performance. Currently, zero-dimensional nanoparticles [24,25], one-dimensional nanowires [26], and two-dimensional nanosheets [27–29] have been utilized as semiconductor channel nanomaterials of FET biosensors. Among which, two-dimensional indium gallium zinc oxide (IGZO) shows the advantages of ease to be scalable and high stability, promising its potential as channel nanomaterial of FET biosensors [30,31]. To this end, the development of a highly sensitive and selective IGZO FET biosensor is expected to achieve highly sensitive detection of bladder tumour-associated biomarkers and realize early diagnosis of bladder cancer.

Herein, we report the fabrication of a highly sensitive and selective IGZO FET biosensor for the detection of bladder cancer nucleic acid biomarker in human urine (Scheme 1). Considering the uniform and smooth structure of IGZO with excellent electrical performance, the single-stranded DNA-functionalized IGZO (ssDNA-IGZO) FET exhibits high sensitivity, specificity and sensing reproducibility in the detection of microRNA-21 (miRNA-21), with an ultralow detection limit of 19.8 amol/L. With the ability to detect trace miRNA-21 in human urine, the IGZO FET biosensors could be employed to effectively differentiate urine samples between bladder cancer patients and healthy donors. Our designed IGZO FET biosensors provide a powerful tool for the development of a nanotechnology platform to achieve early diagnosis of bladder cancer, as well as demonstrate great potential in personal health management.

The fabrication route of IGZO biosensors is schematically illustrated in Fig. S1 (Supporting information). In brief, the source (S) and drain (D) electrodes are fabricated by ultra-violet lithography and thermal evaporation to form patterned metallic electrodes on a 4 in. wafer (Fig. S2 in Supporting information). Then, the IGZO channel was directly deposited on patterned metallic electrodes by a radio frequency sputtering system *via* a shadow mask. The cross-section scanning electron microscopy (SEM) image of the IGZO channel clearly shows a smooth surface and the thickness of IGZO layer is about 20 nm (Fig. 1a), which is consistent with the thickness measured by atomic force microscopy (AFM) (Fig. 1b). After that, the surface of IGZO is passivated with polymethyl methacrylate to minimize gate current leakage, side electrochemical reaction, and work-function modulation. The IGZO sensing area was exposed by electron beam lithography, and further covalently decorated with single-stranded DNA probes to achieve ssDNA-IGZO biosensors.

To identify whether the IGZO biosensors could be used for detecting biomarkers, the fundamental electrical performance of IGZO FET was investigated (Fig. 1, Figs. S3 and S4 in Supporting information). The I_d-V_g transfer characteristic of back-gated IGZO FET presents n-type transistor behavior with a field-effect mobility (μ_{FE}) of 8.3 cm^2 V^{-1} s^{-1} and a current on/off ratio of 10^7 (Fig. 1c). It is worth mentioning that the μ_{FE} of IGZO is relevant to the thickness of the deposited IGZO channel obtained with different sputtering times, and the μ_{FE} of the IGZO channel prepared by 20 min sputtering time reaches the highest μ_{FE} (Figs. S3 and S4). The I_d-V_d output characteristic of the IGZO FET suggests that the μ_{FE} is effectively controlled by V_g (Fig. S5 in Supporting information). To explore the stability of our designed IGZO FETs, eight IGZO FET devices were prepared on a same substrate and the transfer characteristics were recorded (Fig. 1d). It can be seen that the I_d-V_g curves of eight IGZO FETs are highly consistent, indicating that the IGZO FETs exhibit high reliability and performance uniformity. Since bladder cancer biomarkers are presented in body fluid, the electrical performance of IGZO FET in solution environment was investigated. It can be seen that the on-state current and on/off ratio remain almost the same with those of back-gated IGZO FETs (Fig. S6 in Supporting information). The above results demonstrate that the excellent electrical performance of IGZO FET was well maintained, promising their application in highly sensitive and reliable biosensing.

The IGZO FET with outstanding stability and high on/off ratio was designed to construct ultrasensitive biosensors for the detection of bladder cancer associated miRNA-21. To achieve selective detection of bladder cancer biomarkers, the surface of IGZO was covalently modified with single-stranded DNA (ssDNA) that is specific for miRNA-21 with the assistance of linker molecules (Scheme 1, Table S1 in Supporting information), forming ssDNA-IGZO. In order to confirm the feasibility of surface functionalization, we used AFM to analysis the morphology of IGZO FET biosensors before and after probe DNA modification (Figs. 2a and b). It can be seen that the surface of unmodified IGZO is smooth, while the surface roughness of ssDNA-IGZO increased dramatically, indicating that ssDNA probes were successfully fixed on the IGZO surface. In addition, the appearance of characteristic peak of S 2p in the X-ray photoelectron spectroscopy (XPS) curve also proves the successful immobilization of ssDNA probes onto IGZO (Fig. S7 in Supporting information). The successful immobilization of ssDNA probes can be further validated by an obvious I_d drop of IGZO FETs that is originated from the negative gate effect of negatively charged ssDNA molecules (Fig. 2c). The stability of ssDNA-IGZO FET biosensors was investigated by exposing the device in air for a period of time. As shown in Fig. S8 (Supporting information), the I_d of the biosensors almost remains unchanged with prolonged time,

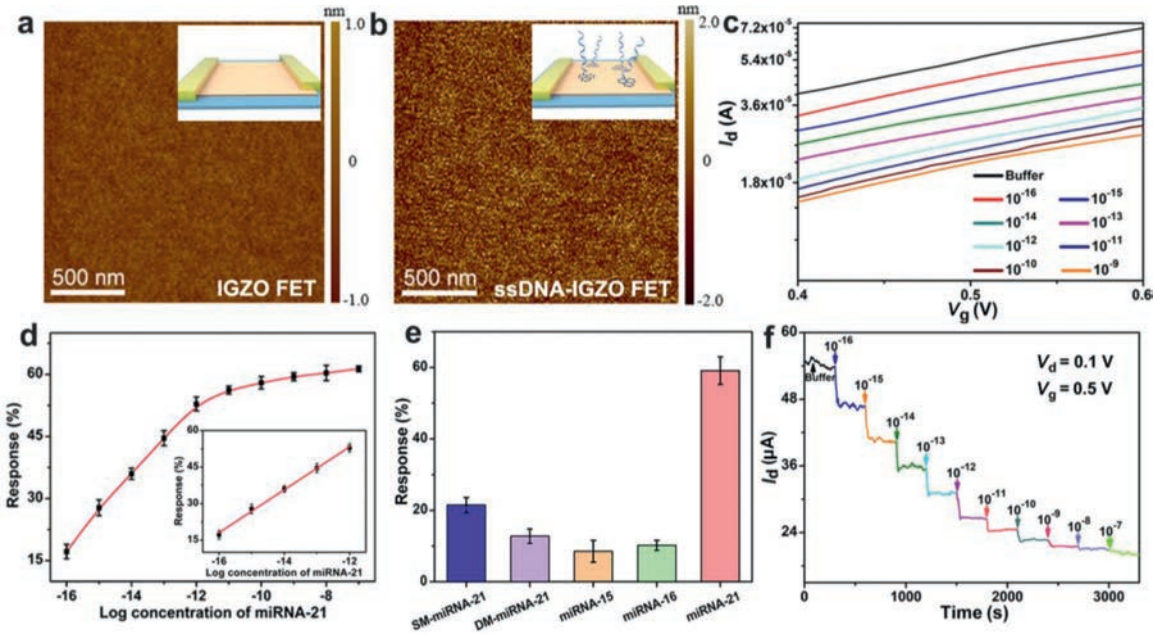

Fig. 2. Detection of miRNA-21 using ssDNA-IGZO FET biosensors. AFM images and schematic diagram of IGZO FETs (a) before and (b) after probe ssDNA modification. (c) Transfer characteristic curves of solution-gated ssDNA-IGZO FET biosensors in response to miRNA-21 with concentrations increase from 10^{-16} mol/L to 10^{-9} mol/L. V_d = 0.1 V. (d) The relationship and (inset of d) the linear curve between the current response of ssDNA-IGZO FET biosensors and the log concentration of miRNA-21 ranging from 10^{-16} to 10^{-7} mol/L. V_g = 0.5 V and V_d = 0.1 V. (e) Selectivity of ssDNA-IGZO FET biosensors toward miRNA-21 (10 pmol/L) and 1 nmol/L of single-mismatched miRNA-21 (denoted as SM-miRNA-21), double-mismatched miRNA-21 (denoted as DM-miRNA-21), miRNA-15 and miRNA-16, respectively. (f) Real-time response of ssDNA-IGZO FET biosensors to different concentrations of miRNA-21. All the error bars represent the standard deviations of three measurements.

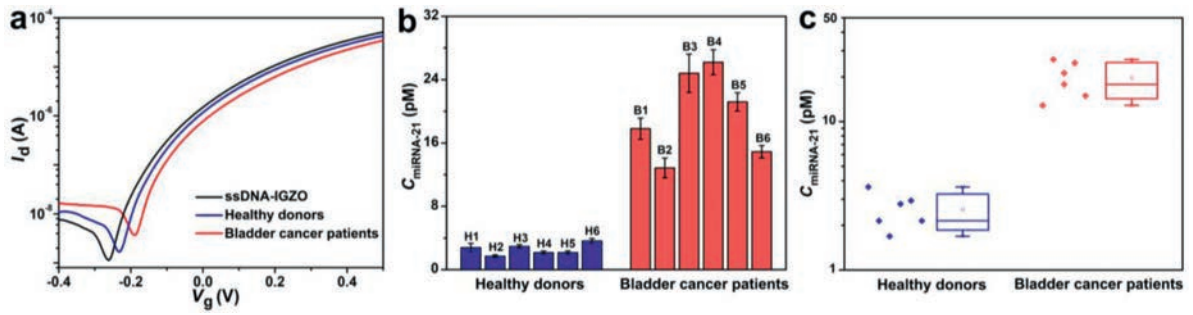

Fig. 3. Detection of human urine samples with ssDNA-IGZO FET biosensors. (a) Transfer characteristics of ssDNA-IGZO FET biosensors in response to miRNA-21 in human urine samples of bladder cancer patients and healthy donors at V_d = 0.1 V. (b) Evaluation of miRNA-21 expression quantity in 6 bladder cancer patients (denoted as B1, B2, B3, B4, B5, B6) and 6 healthy donors (denoted as H1, H2, H3, H4, H5, H6) with ssDNA-IGZO FET biosensors. The error bars represent the standard deviations of three measurements. (c) Statistical analysis of miRNA-21 quantity to differentiate bladder cancer patients and healthy donors.

demonstrating that the ssDNA-IGZO FET biosensors exhibit long-term stability.

Before performing biosensing investigations, the modification parameters of ssDNA including immobilization time and usage amount of ssDNA were investigated (Fig. S9 in Supporting information). As indicated in Fig. S9, the optimized ssDNA modification concentration and the immobilization time is 1 μmol/L and 10 h. Then, the I_d-V_g curves were recorded after incubating the devices with different concentrations of target miRNA-21 for 30 min. As indicated in Fig. 2c, ssDNA-IGZO FET biosensor exhibits a drain current decrease of 7.8 μA upon hybridizing miRNA-21 with a concentration of 10^{-16} mol/L and then shows a consistent decrease in I_d as the concentration of miRNA-21 increases from 10^{-16} mol/L to 10^{-9} mol/L. The decreased drain current can be originated from the accumulation of negative surface charge in n-type IGZO channel upon the binding of negatively charged miRNA-21 chains. In this regard, the binding of negatively charged miRNA-21 is equivalent to negative charge gating of ssDNA-IGZO, resulting in the decrease of I_d. The response of ssDNA-IGZO FET biosensors to miRNA-21 is defined as $\Delta I/I_o$, where ΔI represents the change of I_d before and after miRNA-21 hybridization, and I_o is the initial current of ssDNA-IGZO FET biosensors. Fig. 2d plots the relationship between current response and the logarithm concentrations of miRNA-21. It can be seen that $\Delta I/I_o$ exhibits a linear increase as the concentration of miRNA-21 increases from 10^{-16} mol/L to 10^{-12} mol/L and then gradually reaches saturation above 10^{-12} mol/L (Fig. 2d). According to $3s/\sigma$ criterion (s, standard deviation of 8 blank samples; σ, slope of linear work curve), the detection limit of ssDNA-IGZO FET biosensors is calculated to be 19.8 amol/L, which is much lower than previously reported miRNA detection methods such as fluorescence and electrochemical methods (Table S2 in Supporting information). Furthermore, control experiments were performed to determine the selectivity of ssDNA-IGZO FET biosensors. As shown in Fig. 2e, the current response of ssDNA-IGZO FET biosensor towards an extremely low concentration (10 pmol/L) of miRNA-21 chain is as high as 59.1%. In contrast, the current variation of ssDNA-IGZO FET biosensor is extremely low even when the device was exposed to mismatched miRNA with a high concentration of 1 nmol/L (Table S1). These results indicate that the fabricated ssDNA-

IGZO FET biosensors exhibit high selectivity toward target miRNA-21 over mismatched RNA chains.

The real-time detection was also performed to determine the sensitivity of ssDNA-IGZO FET biosensors (Fig. 2f). Specifically, a series of miRNA-21 with different concentrations was injected onto the surface of ssDNA-IGZO FET biosensors at a fixed rate of 0.1 mL/min. The I_d gradually decreases with continuously injecting of miRNA-21. Particularly, when the solution containing 10^{-16} mol/L miRNA-21 was initially injected, the current decreased by 7.2 μA, which is in highly agreement with the current variation depicted in Fig. 2c. With the increase of the concentration of miRNA-21, the current response decreases due to gradually saturation of hybridized miRNA-21. The fast response speed and high sensitivity of the ssDNA-IGZO FET biosensors provide the possibility for its application in real-time biomarker analysis. The biosensing experiments clearly demonstrate that the ssDNA-IGZO FET with excellent electronic performance could be utilized as high sensitivity and selectivity biosensors for the detection of bladder cancer biomarkers in complex body fluid environment.

To investigate the applicability of IGZO FET biosensors in real urine environments, we first investigated the recovery of spiked miRNA-21 in human urine samples. As shown in Table S3 in Supporting information, the recovery of ssDNA-IGZO FET biosensors ranges from 96.5% to 106.8% when the added miRNA concentration ranges from 10^{-15} mol/L to 10^{-13} mol/L. These results suggest that our IGZO-FET biosensors can be employed to evaluate miRNA-21 molecules in human urine samples. Subsequently, we detected miRNA-21 that is extracted from human urine samples (Fig. S10 in Supporting information). As depicted in Fig. 3a, the current variation of bladder cancer patient samples is significantly higher than that of healthy donors. In order to give a clear comparison, we tested urine samples from different individuals (6 bladder cancer patients and 6 healthy donors, respectively) and then calculated the quantity of miRNA-21 based on the linear curve of $\Delta I/I_0$ *versus* miRNA 21 concentration (Figs. 3b and c). From the calculated results, it can be concluded that the expression level of miRNA-21 in bladder cancer patient samples is much higher than that of healthy donors, which is in accordance with upregulated expression theory reported in literature [32]. These results also clearly indicate that the device could effectively differentiate urine samples between bladder cancer patients and healthy donors. Additionally, the ssDNA-IGZO FET biosensors exhibit excellent reproducibility in eight parallel detections of a same urine sample (Fig. S11 in Supporting information). With the ability to detect low abundance miRNA-21 in human urine samples, the IGZO FET biosensors are expected to detect various kinds of biomolecules or cells in complex environment by functionalizing the corresponding probe molecules on the biosensors.

In conclusion, we developed IGZO FET biosensors with high sensitivity and selectivity to detect trace miRNA in human urine samples. The excellent electrical properties of IGZO FET and the uniform IGZO over large-area enable the high sensitivity and reproducibility of IGZO biosensors. Functionalized modification of specific ssDNA probes endows IGZO FET biosensors with high selectivity for real-time quantification of miRNA-21 with a detection limit of 19.8 amol/L. Particularly, our designed ssDNA-IGZO FET biosensors realize the ultra-sensitive detection of miRNA-21 extracted from human urine and could effectively differentiate urine samples between bladder cancer patients and healthy donors. The development of high stability IGZO FET biosensors opens new opportunities for reliable and efficient diagnosis of early-stage bladder cancer.

Declaration of competing interest

The authors declare no conflict of interest.

Acknowledgments

This work was supported by the National Key Research and Development Program of China (No. 2017YFA0208000), and the Natural Science Foundation of China (Nos. 21904100, 21904033). Yanbing Yang thanks initiatory financial support from Wuhan University.

Supplementary materials

Supplementary material associated with this article can be found, in the online version, at doi:10.1016/j.cclet.2021.07.048.

References

[1] L. Tran, J.F. Xiao, N. Agarwal, J.E. Duex, D. Theodorescu, Nat. Rev. Cancer 21 (2021) 104–121.
[2] J. Huang, Y. Jiang, J. Li, et al., Angew. Chem. Int. Ed. 59 (2020) 4415–4420.
[3] R.M. Davis, B. Kiss, D.R. Trivedi, et al., ACS Nano 12 (2018) 9669–9679.
[4] Y.Y. Broza, R. Vishinkin, O. Barash, M.K. Nakhleh, H. Haick, Chem. Soc. Rev. 47 (2018) 4781–4859.
[5] H. Choi, S.H. Cho, S.K. Hahn, ACS Nano 14 (2020) 6683–6692.
[6] D. Tilki, M. Burger, G. Dalbagni, et al., Eur. Urol. 60 (2011) 484–492.
[7] N. Lobo, C. Mount, K. Omar, et al., Nat. Rev. Urol. 14 (2017) 565–574.
[8] R. Kandimalla, A.A. van Tilborg, E.C. Zwarthoff, Nat. Rev. Urol. 10 (2013) 327–335.
[9] E.S. Martens-Uzunova, R. Bottcher, C.M. Croce, et al., Eur. Urol. 65 (2014) 1140–1151.
[10] M. Frantzi, A. Latosinska, L. Flühe, et al., Nat. Rev. Urol. 12 (2015) 317–330.
[11] Y. Yang, B. Zeng, Y. Li, et al., Sci. China Chem. 63 (2020) 997–1003.
[12] Y. Liu, W. Huang, Z. Cai, Nat. Commun. 11 (2020) 5486.
[13] S.S. Dinges, A. Hohm, L.A. Vandergrift, et al., Nat. Rev. Urol. 16 (2019) 339–362.
[14] H. Yoshino, N. Seki, T. Itesako, et al., Nat. Rev. Urol. 10 (2013) 396–404.
[15] N. Cheng, Y. Xu, Y. Luo, et al., Chem. Commun. 53 (2017) 4222–4225.
[16] H. Peng, A.M. Newbigging, M.S. Reid, et al., Anal. Chem. 92 (2020) 292–308.
[17] M Liang, M. Pan, J. Hu, F. Wang, X. Liu, ChemElectroChem 5 (2018) 1380–1386.
[18] X. Wei, F. Bian, X. Cai, et al., Anal. Chem. 92 (2020) 6121–6127.
[19] A. Zhang, C.M. Lieber, Chem. Rev. 116 (2016) 215–257.
[20] J. Zhang, L.P. Smaga, N.S.R. Satyavolu, J. Chan, Y. Lu, J. Am. Chem. Soc. 139 (2017) 17225–17228.
[21] X. Liu, F. Wang, R. Aizen, O. Yehezkeli, I. Willner, J. Am. Chem. Soc. 135 (2013) 11832–11839.
[22] N. Rohaizad, C.C. Mayorga-Martinez, M. Fojtu, N.M. Latiff, M. Pumera, Chem. Soc. Rev. 50 (2021) 619–657.
[23] C. Cao, J. Zhang, S. Li, Q. Xiong, Small 10 (2014) 3252–3256.
[24] M.K. Masud, J. Na, M. Younus, et al., Chem. Soc. Rev. 48 (2019) 5717–5751.
[25] Y. Wang, Z. Li, Q. Lin, et al., ACS Sens. 4 (2019) 2124–2130.
[26] M.A. Bangar, D.J. Shirale, W. Chen, N.V. Myung, A. Mulchandani, Anal. Chem. 81 (2009) 2168–2175.
[27] A. Lopez, J. Liu, Anal. Chem. 93 (2021) 3018–3025.
[28] M.T. Hwang, M. Heiranian, Y. Kim, et al., Nat. Commun. 11 (2020) 1543.
[29] Y. Yang, X. Yang, X. Zou, et al., Adv. Func. Mater. 27 (2017) 1604096.
[30] K. Nomura, H. Ohta, A. Takagi, et al., Nature 432 (2004) 488–492.
[31] Y. Li, B. Zeng, Y. Yang, et al., Chin. Chem. Lett. 31 (2020) 1387–1391.
[32] R. Duan, Z. Zhang, F. Zheng, et al., ACS Appl. Mater. Interfaces 9 (2017) 23420–23427.